MEASURING FLEXTENSIONAL TRANSDUCER MODE SHAPES UNDERWATER USING LASER SPECKLE INTERFEROMETRY

J N Petzing (1), J R Tyrer (1) & J R Oswin (2)

(1) Loughborough University of Technology, Department of Mechanical Engineering, Loughborough, Leicestershire, UK
(2) BaeSEMA(Marine Division) Ltd., Filton, Bristol, UK

1. INTRODUCTION

Flextensional transducers provide a means of generating high power sound transmissions underwater, in the frequency range of 300Hz to 3000Hz [1]. Early analysis of such units [2] had assumed three principal modes of vibration: the flextensional (Figure 1a), the second flextensional (Figure 1b) and the breathing mode (Figure 1c), and were constant in height. They are not readily amenable to traditional equivalent circuit analysis methods, but Finite Element (FE) techniques [3] have been shown to be successful. More recently, FE analysis has been extended to three dimensional modelling of transducers [4], the results suggesting that the modal structure is not necessarily consistent across the surfaces of the transducers. As in many cases where a modelling technique such as FE is used, experimental verification is generally required for model validation. The displacement maps produced by the software packages cannot be directly related to standard electroacoustic tests and it is wholefield laser speckle pattern interferometry which has been employed to analyse transducer behaviour in air and in water.

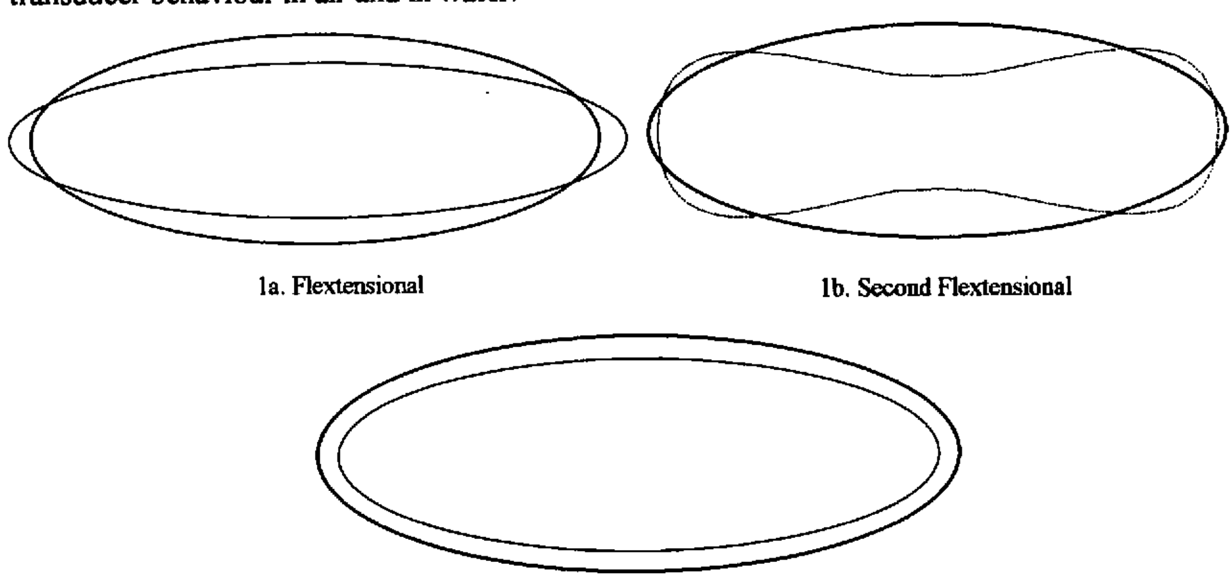

1a. Flextensional

1b. Second Flextensional

1c. Breathing

Figure 1: Flextensional transducer vibration modes

Previous interferometric analysis used Electronic Speckle Pattern Interferometry (ESPI) to represent resonant vibration mode features in terms of correlation interferograms. Experiments were performed in laboratory and in water test facilities [5,6], during which fringe patterns were recorded for subsequent qualitative analysis. Speckle pattern shearing interferometry has recently been adopted as an innovative means of visualising large amplitude ultrasonic component excitation, and overcoming problems encountered during ESPI experimentation. This paper describes measurements of a 3000Hz aluminium alloy shell transducer, showing mode shapes obtained during air and water testing, demonstrating the improvement of data quality obtained through the use of shearing interferometry.

2. ELECTRONIC SPECKLE PATTERN SHEARING INTERFEROMETRY

Previous work has used Electronic Speckle Pattern Interferometry (ESPI) for the examination of transducers in the laboratory and in underwater test facilities, producing wholefield displacement maps describing out-of-plane and in-plane resonant vibration. The speckle physics governing the interferometric technique allow correlation fringe patterns to be formed either via a subtraction process (hardware or software reliant) or an addition process (a function of the image plane recording media). The virtues of these processes were discussed by Oswin *et al* [5,6], presenting correlation fringe patterns describing transducer resonant mode characteristics. The conclusions derived from this work, suggested that wholefield speckle pattern interferometry was potentially a suitable method for examining the resonant characteristics of transducers, whilst in water. However, the quality of the data generated (Figure 2) was dependent on the stability of the transducer, and the associated reference beam optics. The resulting underwater fringe patterns (addition and subtraction) were of poor quality and unsuitable for any post-processing.

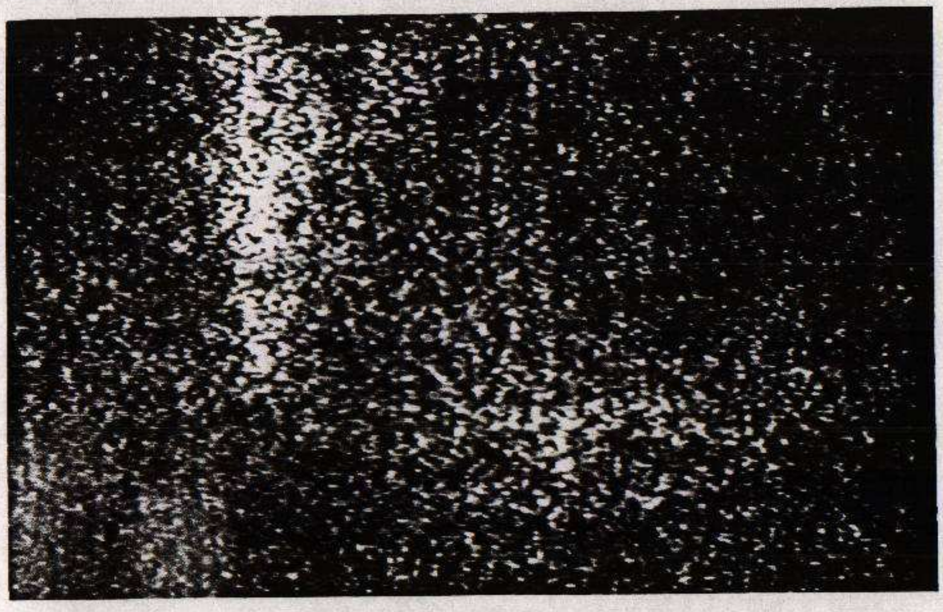

Figure 2: Water based ESPI displacement analysis of a transducer

Further experimental trials have been completed using a different type of speckle interferometer. Laser based Electronic Speckle Pattern Shearing Interferometry (ESPSI) as an experimental technique was initially reported by Leendertz & Butters [7]. Although much development of the interferometer design has taken place over the last twenty years, the optics have been relatively unpopular with respect to other interferometer concepts. Shearing interferometry has generally been restricted to optical shop testing of lenses and mirrors, and used for Non-Destructive Testing (NDT) of fibre reinforced composite panels in the aerospace industry. Some work has been completed, attempting to use shearing interferometry for strain analysis, and a limited amount of dynamic experimentation has been reported (Hung [8]), but in terms of concepts rather than applied experimentation. The reason for the unpopularity is that the correlation fringe interferograms (formed as a product of the laser interferometry) no longer represent lines of isoamplitude, but describe lines of constant displacement gradient (the first spatial derivative of displacement). Consequently, qualitative analysis of displacement gradient functions, be they static, dynamic or transient, is no longer a straight forward intuitive process.

The attraction of the technique is that certain specific interferometer designs incorporate considerable adjustment capabilities, allowing the sensitivity of the analytical equipment to be tuned to the amplitude range of the object being studied. Unlike out-of-plane (OOP) ESPI, a local reference beam is no longer required. Furthermore, the pathlength difference introduced by the optics is very small, hence shearing interferometers do not require large laser temporal coherence lengths, and are less prone to optical noise caused by environmental disturbances such as thermals and vibration.

The work of Leendertz & Butters was based on a Michelson interferometer concept (Figure 3). The interferometer works by superimposing two identical speckle patterns, which are produced when coherent monochromatic laser light illuminates the object surface. Each of the two speckle images is composed of random amplitude and phase distributions, and when combined with a lateral shift δx, produces a unique intensity distribution describing the object surface, a function of the two sets of speckle phases. When a displacement function occurs to the object, the relative phase will cycle through 2π or more. Multiples of 2π will not alter this state at the respective point, but submultiples cause changes of point intensities, seen as correlation fringes.

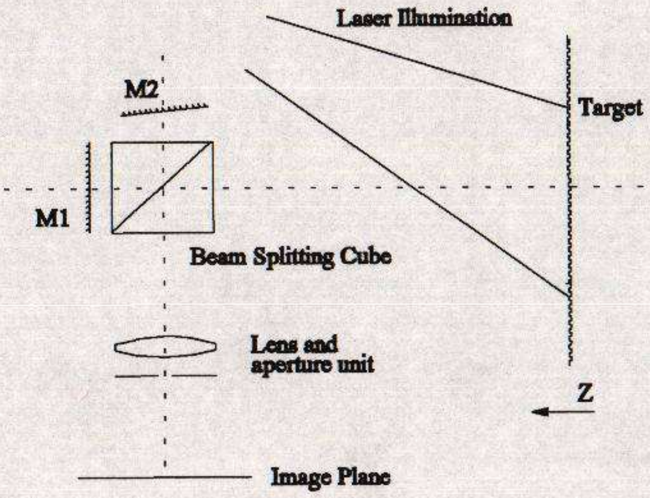

Figure 3: Speckle shearing interferometer design

Correlation fringes are formed by electronic subtraction (in real-time), the fringes representing contours of constant gradient displacement - dw/dx. For dynamically generated displacements, a Bessel function modulates the correlation fringes (if using a Continuous Wave laser) resulting in a modified intensity of fringe contrast from the regions of zero difference. This causes a rapid deterioration of fringe visibility, reducing the displacement gradient step size which the interferometer can view in one operation. Furthermore, the inclusion of the Bessel function modifies the fringe structure to an extent where quantitative data can no longer be extracted from the interferograms. Hence 'time-averaged' Bessel function fringes are generally only suitable for qualitative analysis of dynamic object behaviour and it is necessary to use a pulsed laser to remove the modulating function. In this case, the correlation fringes are cosinusoidal in nature, allowing the use of quasi-heterodyning techniques to be used to extract quantitative data from the interferograms.

3. EXPERIMENTAL DETAILS

The transducer was a 3kHz aluminium shelled transducer (Figure 4) with two ceramic stacks, each comprising 20 Navy III ceramic plates (40mm x 20mm x 5mm), with Steatite insulators. The main dimensions of these units were; semi-major axis 75mm, semi-minor axis 28mm, wall thickness 16mm, height 100mm; with the axes measured from the centre of the transducer to the centre line of the shell wall. The transducer was initially examined in air using OOP ESPI and OOP ESPSI. ESPI was necessary to provide a broad understanding of the object behaviour in terms of recognisable displacement resonant modes, allowing later shearing fringe interferograms to be interpreted. A commercial Vidispec (Ealing Optics) interferometer (632.8nm) was used in this instance, with data recorded onto videotape via an image processing computer, for subsequent analysis. The ESPSI experimentation was conducted in two parts. Firstly, a CW argon ion (514nm) laser illuminated the object, then the experimentation was repeated using a pulsed laser.

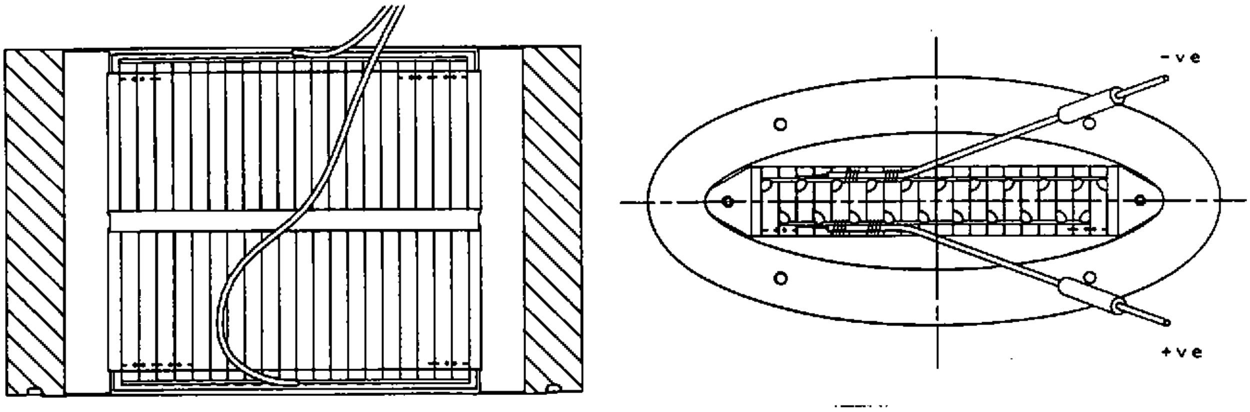

Figure 4: Schematic of the 3kHz transducer

The pulsed shearing interferometer utilised a Spectron Nd:YAG single pulse laser (max. 30mJ), frequency doubled to 532nm, with a maximum repetition rate of 25Hz. Using pulse generators and synchronisation circuits, the laser was synchronised to the CCD TV camera, such that the pulse repetitively illuminated the first field of each frame. Furthermore, the nature of the electronics ensured that the laser pulses illuminated the transducers at the same point on the oscillatory cycle or waveform. Different parts of the waveform could be examined by altering the delay between the firing cycle of the Q-switched laser and the sinusoidal excitation frequency, in terms of subtraction correlation fringes, produced by the same equipment used for the CW experimentation. The short duration of the Nd:YAG laser pulses overcame the 'time-average' effect experienced by the CW interferometers, presenting the displacement derivative data in terms of cosinusoidal fringes, instead of Bessel function modulated interferograms.

A broad understanding of the transducer characteristics was developed in the laboratory, identifying the main resonant modes of importance, their spatial structure and frequency of operation in air. Transducer excitation was achieved using an HP3330A digital frequency synthesiser with amplifier, incrementally sweeping through a frequency range of 500Hz to 15,000Hz, pausing and optimising as each resonant mode was discovered. In all cases the vertical and horizontal displacement derivative components were examined using ESPSI, with lateral shear values of δx=5%. The second part of the experimentation involved repeating the laboratory based testing with the transducer immersed in a large water tank (10m x 6m x 6.5m). The details of the facility are shown in Figure 5. The transducer was suspended from a crane located above the tank, and positioned 2m away from one of the upper tank viewing windows. The laser, optics, excitation and recording equipment were housed in the viewing gallery, with the laser and optics illuminating and examining the transducer through the window. The experimentation proceeded as before, with the transducer excited through the frequency range 500Hz to 15,000Hz, whilst examining the vertical and horizontal displacement derivative components.

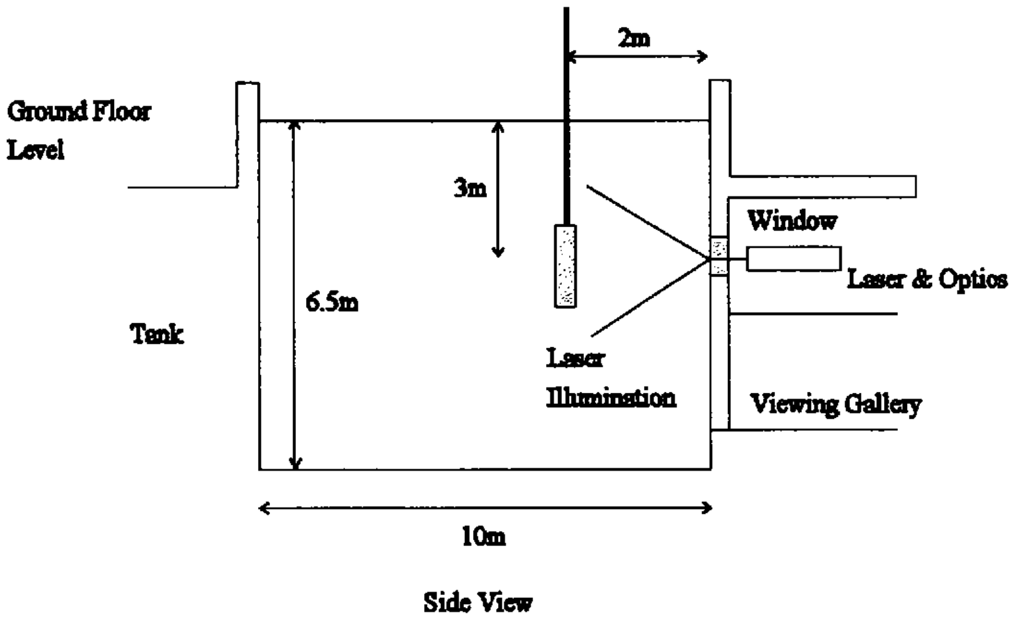

Figure 5: Schematic showing underwater test facilities

4. RESULTS AND DISCUSSION

4.1 Laboratory based experimentation

The laboratory experimentation used the out-of-plane displacement interferometer to provide a set of reference images. Figure 6 shows a time-averaged OOP displacement fringe pattern, describing the shell motion of the transducer at 4260Hz (5V). The resonant mode is composed of one anti-node. Fringes can be seen, but contrast alters drastically as the number of fringes in the anti-node increases, a consequence of the zero order Bessel function. Whilst extraction of quantitative data from these images is not possible, by fringe counting an estimate of the peak-peak amplitude of the anti-node can be generated.

The OOP ESPI interferometer was replaced with an OOP shearing interferometer, using CW illumination of the transducer. The previous experimentation was repeated although more emphasis was placed on optimising the shearing optics. Figure 7 (4240Hz, 10V) demonstrates a typical time-averaged subtraction correlation shearing interferogram obtained from this testing, visualising the same resonant mode as depicted in Figure 6. There is much similarity between the two figures although there is now one central nodal regions (white vertical band) and two anti-nodes either side. The increase in the number of these features is a function of the data which the fringes represent. As already explained above, shearing interferometers visualise displacement gradients or slope rather than displacement. If a geometric analysis is performed of the fringes shown in Figure 7 the slope changes can be deduced. Regions of zero displacement (nodal regions) are of constant slope whilst the amplitude peaks (anti-nodes) contain very little or zero slope change. This subtle difference can cause confusion when interpreting shearing interferograms, the understanding of which is not as intuitive as ordinary out-of-plane displacement fringes.

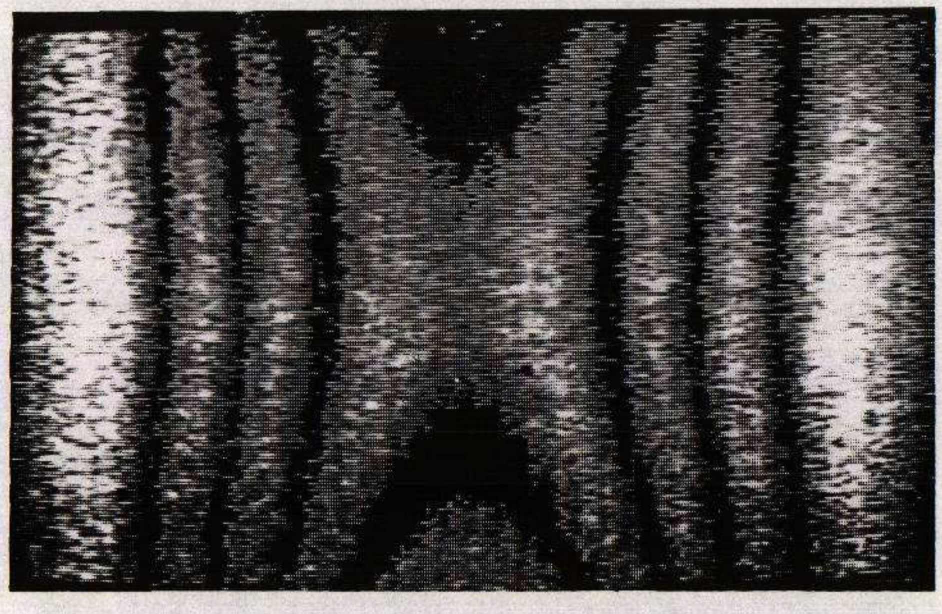

Figure 6: Time-averaged displacement fringe pattern

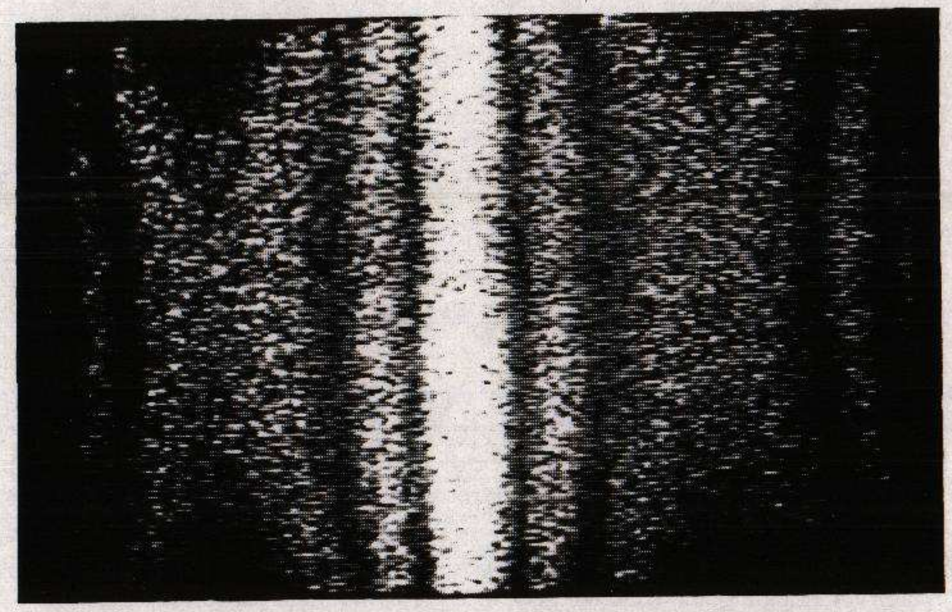

Figure 7: Time-averaged shearing fringe pattern

It is clear that the time-averaged shearing fringes are of similar quality to the displacement data, with fringe contrast limited by the modulating Bessel function. Previous work [9] has shown that altering the sensitivity of the interferometer for large displacement functions can to some extent alleviate the problem, but the data still remains of qualitative interest only. As in the case of ESPI, pulsed laser illumination is required in order to produce fringe patterns which can be post-processed using image-processing techniques.

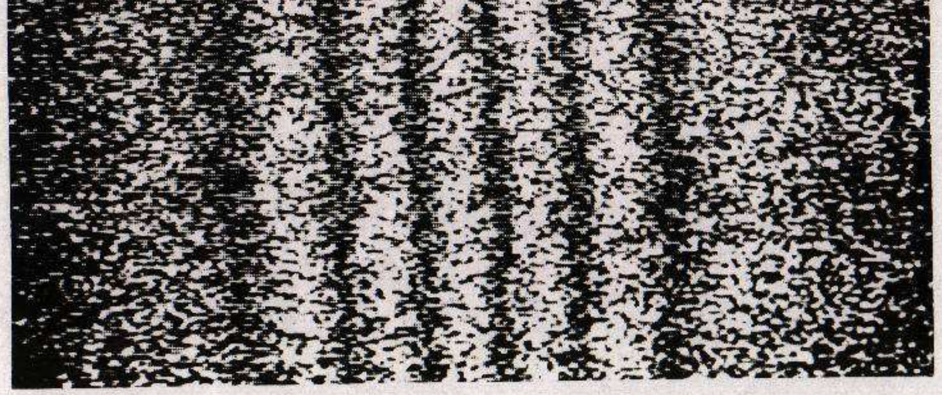

Figure 8: Pulsed shearing interferogram of a transducer vibration mode

The pulsed equivalent of Figure 7 is shown in Figure 8 (4240Hz, 10V). The two anti-nodes are visible (but with reduced contrast) at the sides of the image, with the nodal region apearing in the middle.The nodal region does not appear as a broad white region in this case because the cosinusoidal pulsed fringes are not modulated by the Bessel function. Deterioration of the data contrast is caused by the extent of the lateral shear of the interferometer, and the rapidly curving surface of the transducer at its extremities. Reducing the lateral shear improves the outer fringe contrast but reduces the interferometer sensitivity, hence a compromise was reached between lateral shear and fringe visibility.

4.2 Underwater experimentation

The laboratory experimentation determined the frequencies and resonant behaviour of the transducer in air, and confirmed the ability of pulsed ESPSI to visualise the resonant mode shapes. Experimentation was repeated with the transducer placed in the large underwater testing facility at BAeSEMA, with the pulsed interferometer positioned in a subsurface viewing gallery.

Water based resonant mode frequency values have been collated and are presented in Table 1 with the equivalent in-air laboratory results. Operating frequencies are highlighted in bold text, and the mode shapes are identified as a,b, or c with respect to Figure 1. The larger apparent number of resonant frequency values observed during the tank tests can be attributed to acoustic standing waves within the tank facility. Ideally the measurements should be conducted in an infinite expanse of water, or the transducer should be operated with very short pulse excitation (rather than continuous wave) and switched off before reflections occur, typically within 2ms. The frequency values are notably lower than the air experiments, caused by the mass loading effect of the water; i.e. the

In-Air Frequency (Hz)	Underwater Frequency (Hz)
4240 (a)	**2990 (a)**
4345	3040
14145	3190
15850 (c)	3860
	9800
	11570 (c)

Table 1: Transducer resonant frequency values

imaginary component of the acoustic load. The fringe patterns displayed similar spatial structure, although with less variability over the height of the structure. The quality of the fringes (Figure 9) is only slightly poorer than the laboratory data shown in Figure 8, and in a similar fashion, the two antinodes have reduced contrast. Strong specular reflection of laser light was obtained from the minor axis of the transducers which caused saturation of the CCD camera, reducing the effectiveness of the interferometer. This problem was overcome by spraying the transducers matt white and reducing the laser power, although this reduced the optical signal-to-noise ratio across the whole of the image.

In general, the mode shapes observed in water differed slightly from those in air, the spatial form of the fringes being straighter and more upright for the water results. The extent of the differences visualised with the speckle shearing interferometer were similar to the information derived from previous ESPI studies [5-6], although the quality of the underwater shearing interferograms far exceeded previous trial data.

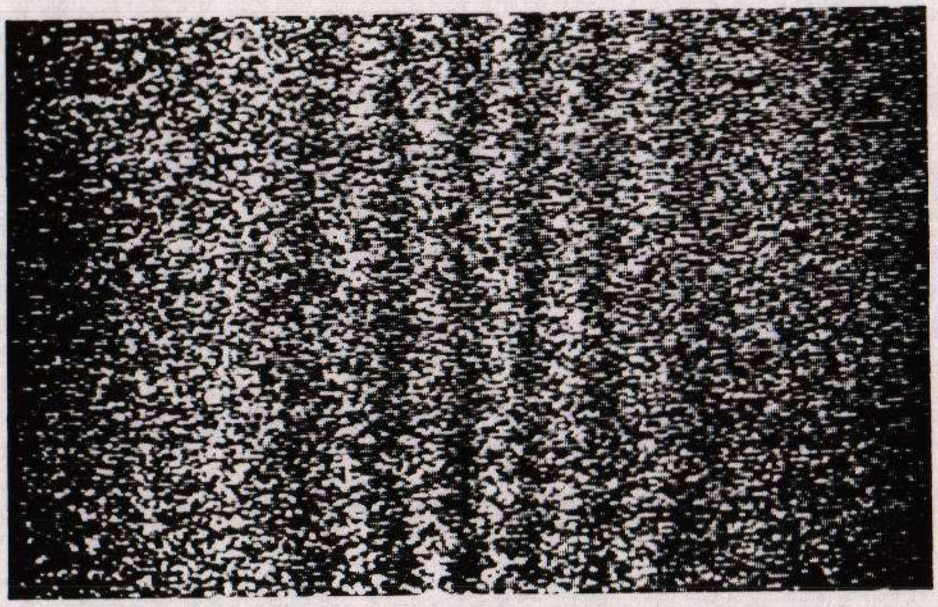

Figure 9: Shearing fringes on a transducer, whilst in water

5. CONCLUSIONS

Experimental wholefield laser analysis of flextensional transducers can be described as routine if the testing is performed in a laboratory, but similar information concerning transducer behaviour whilst underwater has been much more difficult to obtain. Previous work using ESPI showed potential, but the data was very poor and did not allow any form of post-processing.

This series of experiments has taken a related laser interferometric technique - ESPSI, and applied it in the laboratory and in underwater conditions. The laboratory results demonstrated that speckle shearing interferometry was capable of visualising transducer resonant vibration modes across a frequency range of 0Hz - 15,000Hz, although the fringe pattern data represented lines of constant displacement gradient or slope, unlike the displacement fringes produced by ESPI. Furthermore, adjustment of the amount of lateral shear applied to the interferometer can optimise the optical sensitivity to the boundary conditions of the object under test.

The underwater experimentation has shown ESPSI to be suitable for the generation of wholefield interferometric data from transducers, whilst operating in their working environment. This allows the transducer designers to better understand the dynamics of the units and to fully verify Finite Element models. The experimental data has shown that the frequency of resonance decreases when the transducers operate in water and the spatial characteristics of the resonant modes are slightly different to the in-air tests. In all cases, the quality of the correlation interferograms has been sufficient to allow computer based post-processing of the data. Furthermore, this successful and unique application of wholefield speckle interferometry could be extended to many other analysis cases, requiring in-situ underwater experimentation and operation.

6. ACKNOWLEDGEMENTS

The work described in this paper was jointly funded by Loughborough University of Technology and BAeSEMA, Filton, Bristol. Experimentation was performed using laboratories at Loughborough University of Technology, and underwater testing facilities at BAeSEMA, with laser equipment supplied by Spectron Lasers, Rugby. The authors wish to thank Mr. V. Scothern and Mr. S. Penney for their technical assistance. The work performed by Researchers at Loughborough, was completed under the auspices of European Community BRITE Contract BRE2 - CT92 - 0332.

7. REFERENCES

[1] J R OSWIN, 'Class IV Flextensional transducers. Modelling, measurement and use', *Proceedings of the First European Conference on Underwater Acoustics,* Luxembourg, In Weydert (ed.), p627-630, Reed-Elsevier, (1992)

[2] J R OSWIN & A TURNER, 'Design limitations of Class IV aluminium shell flextensional transducers', *Proceedings of the Institute of Acoustics,* 6(3) p94-101 (1984)

[3] G A BRIGHAM, 'Analysis of Class IV flextensional transducers by wave mechanics', *Journal of the Acoustical Society of America,* 56(1) p31-39 (1974)

[4] R J BRIND, 'Finite Element Modelling of the ARE low frequency flextensional transducer', *Proccedings of the Institute of Acoustics,* 10(9) p105-128 (1988)

[5] J R OSWIN, 'Underwater laser interferometric measurement of flextensional transducers, MEP', *Proceedings of Undersea Defence Technology,* p707-712 (1992)

[6] J R OSWIN, P L SALTER, F. MENDOZA SANTOYO & J R TYRER, 'Electronic speckle pattern interferometric measurement of flextensional transducer vibration patterns: in air and water', *Journal of Sound and Vibration,* 172(4) p433-448 (1994)

[7] J A LEENDERTZ & J N BUTTERS, 'An image shearing speckle pattern interferometer for measuring bending moments', *Journal of Physics E,* 6 p1107-1110 (1973)

[8] Y Y HUNG & C E TAYLOR, 'Measurement of slopes of structural deflections by speckle shearing interferometry', *Experimental Mechanics,* p281-285 (July 1974)

[9] J N PETZING & J R TYRER, 'Shearing interferometry for power ultrasonic vibration analysis', Lisbon, Portugal, *Proceedings of the 10th International Conference on Experimental Mechanics,* J F Silva Gomes et al (eds.), Balkema, Netherlands, p631-636 (July 1994)